Multichannel Restoration of Single Channel Images Using a Wavelet-Based Subband Decomposition

Mark R. Banham, *Member, IEEE,* Nikolas P. Galatsanos, *Member, IEEE,*
Hector L. Gonzalez, *Member, IEEE,* and Aggelos K. Katsaggelos, *Senior Member, IEEE*

***Abstract*— In this paper, we present a new matrix vector formulation of a wavelet-based subband decomposition. This formulation allows for the decomposition of both the convolution operator and the signal in the subband domain. With this approach, any single channel linear space-invariant filtering problem can be cast into a multichannel framework. We apply this decomposition to the linear space-invariant image restoration problem and propose a family of multichannel linear minimum mean square error (LMMSE) restoration filters. These filters explicitly incorporate both *within* and *between* subband (channel) relations of the decomposed image. Since only within channel stationarity is assumed in the image model, this approach presents a new method for modeling the nonstationarity of images. Experimental results are presented which test the proposed multichannel LMMSE filters. These experiments show that if accurate estimates of the subband statistics are available, the proposed multichannel filters provide major improvements over the traditional single channel filters.**

I. Introduction

RESTORATION is an image processing operation that is frequently applied to degraded image data in order to facilitate other image processing tasks. Examples of such tasks include image recognition and image understanding, which can be performed either automatically by computer, or directly by human observers. Image restoration is a mature research field which has evolved tremendously over the last 20 years. An overview of the recent developments in this field and an extensive list of references can be found in [1].

Based on the model that is used to introduce prior knowledge about the original image, restoration algorithms may be classified into two categories: algorithms that use space-invariant (stationary) models, and algorithms that use space-variant (nonstationary) models. The use of stationary image models is justified by the simplification that they provide to the unmanageable computational load of many restoration algorithms. In spite of this, space-invariant models are an oversimplification of the nature of real images. Therefore, whenever they are used, the restored images suffer from the smoothing of sharp edges, "ringing" artifacts in the vicinity of edges, and noise enhancement in smooth areas of the image.

Many types of space-variant image restoration algorithms have been previously proposed. Some examples include algorithms that incorporate the properties of the human visual system (HVS), and recursive restoration algorithms based on the Kalman filter (see, for example, [2]–[6]). In [7] a local decision process was proposed to switch between different AR models, capturing the orientation of the edges present at different spatial locations. In [8], an AR model was used which was driven by white noise with a space-variant variance to model the residual image. Maximum *a posteriori* probability (MAP) methods have also been proposed for nonstationary image restoration. These methods utilize space-variant density functions as prior knowledge to capture the nonstationarity of the original image. In [1], [9]–[11], doubly-stochastic Markov random fields were used as prior densities, and stochastic relaxation was used to minimize the nonconvex objective function associated with the restoration problem.

In this paper, we present a new matrix formulation of the wavelet-based subband decomposition. This formulation allows for the computation of the decomposition of both the signal and the convolution operator in the subband domain. This permits the conversion of any linear single-channel space-invariant filtering problem to a multichannel one. Subband decomposition is a widely used method for compression of images [12]. The main advantage of this approach is that it allows for the adaptation of the compression algorithm to the properties of each subband separately. Recently, however, there have been a number of studies in the area of image restoration also using subband or wavelet-based approaches [13]–[15]. The motivation for these studies was to capitalize on subband decompositions in a similar fashion to image compression case. In other words, the goal of these techniques was to adapt the restoration algorithm to the properties of the signal, the noise, and the visibility of each subband. However, for most of these investigations, the solutions have either followed independent subband assumptions, or have under-utilized the correlations that exist between subbands in such decompositions. In the proposed approach, since the convolution operator can be decomposed in the subband domain, cross-subband (channel) relations in the observed data can be explicitly taken into account. Therefore, we propose a multichannel linear minimum mean square error (LMMSE)

Manuscript received June 16, 1993; revised June 6, 1994. This work was supported by a grant from the Space Telescope Science Institute and by Grant no. MIP-9309910 from the National Science Foundation. The associate editor coordinating the review of this paper and approving it for publication was Prof. Rama Chellappa.

M. R. Banham is with the Digital Technology Research Laboratory, Motorola Corporate Research and Development, Schaumburg, IL 60196 USA.

N. Galatsanos and H. Gonzalez are with the Department of Electrical and Computer Engineering, Illinois Institute of Technology, Chicago, IL 60616 USA.

A. K. Katsaggelos is with the Department of Electrical Engineering and Computer Science, Robert R. McCormick School of Engineering and Applied Science, Northwestern University, Evanston, IL 60208-3118 USA.

IEEE Log Number 9404447.

restoration filter to simultaneously restore the multiple channels of the decomposed image, much like the approach to color image restoration followed in [16], [17]. Furthermore, a multichannel image model is used that explicitly incorporates both within and between-channel relations of the decomposed original image. Since the only stationarity assumed in this model is that *within* the channels, this approach provides a framework for a family of nonstationary restoration algorithms. For this approach, because the number of channels in the decomposition may vary, one has the flexibility to specify a restoration algorithm in which stationarity and computational complexity can be traded-off.

The linear space-invariant model used here is given by

$$g = Hf + n \tag{1}$$

where H is a circular convolution operator, a circulant matrix, and g, f and n are the observed, original, and noise signals, respectively [18]. A subband decomposition can be used to transform (1) into a domain where g, f, and n are decomposed into channels based on their local frequency content, and the convolution operator H is decomposed into a set of convolution operators that are applied within and between each of these channels separately. This idea will be the starting point for the analysis which follows.

In Section II, multichannel linear filtering and the matrix structures associated with this problem are reviewed. The wavelet-based 1-D subband multichannel decomposition of a signal and convolution operator is presented in Section III. The 1-D decomposition is used to explain the basic idea of this approach in a straightforward manner. In Section IV, this idea is extended to the 2-D case by applying the previously presented decomposition in both the horizontal and vertical directions separately. Using this decomposition, in Section V we present multichannel LMMSE restoration of single-channel images in the subband domain. Finally, in Sections VI and VII, we present experimental results and conclusions, respectively.

II. Multichannel Linear Filtering Matrix Structures

Multichannel linear filtering, as used in this paper, refers to a multiple-input multiple-output linear system [19]. For this system, different linear space-invariant operators are applied to each input to produce each output. Assume a system with P inputs and outputs. Let f_i, g_i, for $i = 1, 2, \ldots P$ be $N \times 1$ vectors, which are inputs and outputs of a multichannel system, respectively. If the multichannel input vector f is given by

$$f = [f_1(0) \cdots f_1(N-1); f_2(0) \cdots f_2(N-1); \ldots; f_P(0) \cdots f_P(N-1)]^T \tag{2}$$

where ^{T} indicates the transpose, and g the output is also given by a similar equation, then the input-output relation of this system may be given by

$$g = \tilde{\mathbf{A}} f \tag{3}$$

where

$$\tilde{\mathbf{A}} = \begin{bmatrix} A_{1,1} & A_{1,2} & \ldots & A_{1,P} \\ A_{2,1} & A_{2,2} & \ldots & A_{2,P} \\ \ldots & \ddots & \ddots & \ldots \\ A_{P,1} & A_{P,2} & \ldots & A_{P,P} \end{bmatrix} \tag{4}$$

and $A_{i,j}$ is an $N \times N$ circulant matrix, for $1 \leq i, j \leq P$. This $PN \times NP$ matrix will be referred to as block-semi circulant (BSC) of order (P, N) [20] and has been previously encountered in multichannel image restoration problems.

A dual and equivalent representation of this multichannel linear system can be obtained if the input and the output are arranged in an interlaced fashion. If f_I, the multichannel input, is given by

$$f_I = [f_1(0), f_2(0), \ldots f_P(0); f_1(1), f_2(1), \ldots f_P(1); \ldots; f_1(N-1), f_2(N-1), \ldots f_P(N-1)]^T \tag{5}$$

and g_I is defined in a similar manner, then the linear multichannel system may be described by

$$g_I = \mathbf{A} f_I \tag{6}$$

with

$$\mathbf{A} = \begin{bmatrix} A_{0,0} & A_{0,1} & \ldots & A_{0,N-1} \\ A_{0,N-1} & A_{0,0} & \ldots & A_{0,N-2} \\ \ldots & \ddots & \ddots & \ldots \\ A_{0,1} & A_{0,2} & \ldots & A_{0,0} \end{bmatrix} \tag{7}$$

where $A_{0,j}$, for $0 \leq j \leq N-1$, is an arbitrary $P \times P$ matrix. This $NP \times PN$ matrix will be referred to as semi-block circulant (SBC) of order (P, N) [20], [21].

It has been shown that SBC and BSC matrices are closed under addition, multiplication, and inversion, and furthermore, that fast computation of these operations may be executed in the discrete Fourier transform (DFT) domain. In the DFT domain, BSC (P, N) matrices are transformed into $PN \times NP$ block matrices that contain P^2 diagonal matrices of size $N \times N$. Equivalently, SBC (P, N) matrices in the DFT domain are transformed into $NP \times PN$ block matrices that contain N^2 $P \times P$ matrices. These $P \times P$ matrices are all zero matrices except for the N matrices along the diagonal. Both of these matrix structures may thus be represented as sparse, and computations with them are fast and efficient [20], [22].

III. Multichannel Decomposition of 1-D Signals and Convolution Operators

The decomposition of a 1-D signal into two channels may be accomplished by the filter bank, which is illustrated in Fig. 1 [23]. Here each filtered signal is decimated by two, such that the total number of samples in the input and output signals is preserved.

We can refer to a matrix representation of this linear system in terms of the ordering of the output channel vectors. It will be easiest to first consider the matrix structure which is used to multiply the original data, without any reordering. This input-output relation may be given in terms of an SBC $(2, \frac{N}{2})$ matrix as

$$Wf = \tilde{f}_I \tag{8}$$

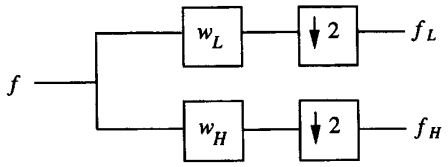

Fig. 1. The two-channel 1-D decomposition.

where f is an $N \times 1$ vector containing the samples of the input signal, and W is an $N \times N$ system matrix. If $w_L(i)$ and $w_H(i)$ represent the coefficients of the impulse responses of the linear space-invariant low and highpass filters used in this filter bank, then for circulant convolutions, W is given by (9) at the bottom of this page, which is SBC(2, $\frac{N}{2}$). The output signal $\tilde{f}_I$ contains the samples of the low and the highpass decimated signals, in an interlaced fashion, as in (5). Assuming that N is even, $\tilde{f}_I$ is given by

$$\tilde{f}_I = \Big[f_L(0), f_H(0),\ f_L(1),\ f_H(1) \ \ldots f_L\Big(\frac{N}{2}-1\Big),\ f_H\Big(\frac{N}{2}-1\Big)\Big]^T. \tag{10}$$

As explained previously, computations involving the W matrix may be performed very efficiently in the DFT domain [21]. Now let us examine the dual case, again placing our reference on the ordering of the output vector. Defining a "deinterlacing" $N \times N$ matrix D by

$$D = \begin{bmatrix} 1&0&0&0&\cdot&\cdot&0&0 \\ 0&0&1&0&\cdot&\cdot&0&0 \\ 0&0&0&0&\cdot&\cdot&0&0 \\ \cdot&\cdot&\cdot&\cdot&\cdot&\cdot&\cdot&\cdot \\ \cdot&\cdot&\cdot&\cdot&\cdot&\cdot&\cdot&\cdot \\ 0&0&0&0&\cdot&\cdot&0&0 \\ 0&0&0&0&\cdot&\cdot&1&0 \\ 0&1&0&0&\cdot&\cdot&0&0 \\ 0&0&0&1&\cdot&\cdot&0&0 \\ \cdot&\cdot&\cdot&\cdot&\cdot&\cdot&\cdot&\cdot \\ \cdot&\cdot&\cdot&\cdot&\cdot&\cdot&\cdot&\cdot \\ 0&0&0&0&\cdot&\cdot&0&0 \\ 0&0&0&0&\cdot&\cdot&0&1 \end{bmatrix} \begin{matrix} 0 \\ 1 \\ 2 \\ \cdot \\ \cdot \\ \cdot \\ N/2-1 \\ N/2 \\ \cdot \\ \cdot \\ \cdot \\ N-2 \\ N-1 \end{matrix} \tag{11}$$

it is easy to see that

$$D\,D^T = D^T D = I,\ D\,f = f_D, \text{ and } D\,\tilde{f}_I = \tilde{f} \tag{12}$$

where I is the $N \times N$ identity matrix,

$$f_D = [f(0),\ f(2), \ldots f(N-2); \ f(1),\ f(3), \ldots f(N-1)]^T \tag{13}$$

and

$$\tilde{f} = \Big[f_L(0),\ f_L(1), \ldots f_L\Big(\frac{N}{2}-1\Big); \ f_H(0),\ f_H(1), \ldots f_H\Big(\frac{N}{2}-1\Big)\Big]^T = [\ {f_L}^T,\ {f_H}^T\ ]^T \tag{14}$$

where f_L and f_H are $\frac{N}{2} \times 1$ vectors containing the ordered samples of the decimated low and highpass output signals, respectively. Equation (14) has the same ordering as (2), where the spatial index changes before the channel index.

Based on the previous definitions, (8) yields

$$(D\ W\ D^T)\ (D\ f) = (D\ \tilde{f}_I) \Longrightarrow \tilde{W}\ f_D = \tilde{f} \tag{15}$$

with $\tilde{W}$ given by

$$\tilde{W} = \begin{bmatrix} {W^E}_L & {W^O}_L \\ {W^E}_H & {W^O}_H \end{bmatrix} \tag{16}$$

where for $i = L, H$

$${W^E}_i = \begin{bmatrix} w_i(0) & w_i(2) & \cdot & w_i(N-2) \\ w_i(N-2) & w_i(0) & \cdot & w_i(N-4) \\ \cdot & \cdot & \cdot & \cdot \\ \cdot & \cdot & \cdot & \cdot \\ w_i(2) & \cdot & w_i(N-2) & w_i(0) \end{bmatrix} \tag{17a}$$

and

$${W^O}_i = \begin{bmatrix} w_i(1) & w_i(3) & \cdot & w_i(N-1) \\ w_i(N-1) & w_i(1) & \cdot & w_i(N-3) \\ \cdot & \cdot & \cdot & \cdot \\ \cdot & \cdot & \cdot & \cdot \\ w_i(3) & \cdot & w_i(N-1) & w_i(1) \end{bmatrix}. \tag{17b}$$

The matrices W_i^j, for $i = L, H$ and $j = O, E$, are $\frac{N}{2} \times \frac{N}{2}$ circulant matrices. However, since $W_L^E \neq W_H^O$, the matrix $\tilde{W}$ does not have a circulant structure, in fact it is BSC $(2, \frac{N}{2})$.

In order to use $\tilde{W}$ as the transformation for the multichannel decomposition of single channel problems, this operator must be easy to define, and $\tilde{W}^{-1}$ must be easy to compute. If w_L and w_H, in Fig. 1, are selected to be quadrature mirror filters (QMF)'s which are based on the orthonormal wavelet bases

$$W = \begin{bmatrix} w_L(0) & w_L(1) & w_L(2) & w_L(3) & \cdot & \cdot & w_L(N-2) & w_L(N-1) \\ w_H(0) & w_H(1) & w_H(2) & w_H(3) & \cdot & \cdot & w_H(N-2) & w_H(N-1) \\ w_L(N-2) & w_L(N-1) & w_L(0) & w_L(1) & \cdot & \cdot & w_H(N-4) & w_H(N-3) \\ w_H(N-2) & w_H(N-1) & w_H(0) & w_H(1) & \cdot & \cdot & w_H(N-4) & w_H(N-3) \\ \cdot & \cdot & \cdot & \cdot & \cdot & \cdot & \cdot & \cdot \\ \cdot & \cdot & \cdot & \cdot & \cdot & \cdot & \cdot & \cdot \\ \cdot & \cdot & \cdot & \cdot & \cdot & \cdot & \cdot & \cdot \\ w_L(2) & w_L(3) & \cdot & \cdot & \cdot & \cdot & w_L(0) & w_L(1) \\ w_H(2) & w_H(3) & \cdot & \cdot & \cdot & \cdot & w_H(0) & w_H(1) \end{bmatrix} \tag{9}$$

with compact support [24], one set of coefficients may be used to define both filters [23]. Furthermore, $\tilde{W}^{-1}$ will simply equal $\tilde{W}^T$, and thus it, along with $\tilde{W}$, may be implemented with FIR filters. In addition, wavelet filters provide a means to compute a regular multiresolution analysis over many levels of decomposition. Thus, the choice of these filters is very convenient, but is not essential for the development of this paper. Since $\tilde{W}$ is a BSC $(2, \frac{N}{2})$ matrix, any nonsingular $\tilde{W}$ can be used. However, the use of the perfect reconstruction wavelet bases makes the analysis more straightforward, and so for the rest of this paper we will assume that $\tilde{W}$ is an orthonormal matrix.

The circulant convolution operator, H, in (1), may be decomposed with either the SBC or BSC representation of the filtering matrix, that is, (9) or (16). Ignoring the noise term for the moment, the convolution operation can be transformed into the W domain by

$$g = Hf \Longrightarrow Wg = WHW^TWf \Longrightarrow \tilde{g}_I = WHW^T\tilde{f}_I. \tag{18}$$

In this case, it is straightforward to observe that the term WHW^T is an SBC $(2, \frac{N}{2})$ matrix since it is the product of three SBC $(2, \frac{N}{2})$ matrices. This is a result of the fact that the circulant matrix H is also an SBC matrix of order $(2, \frac{N}{2})$. Thus, the computation of this term in the discrete frequency domain is straightforward, as discussed in Section II.

In the same way, we can transform convolution into the $\tilde{W}$ domain using the BSC formulation. In this case, (1) yields

$$g = Hf \Longrightarrow (\tilde{W}D)g = (\tilde{W}D)H(D^T\tilde{W}^T)(\tilde{W}D)f. \tag{19}$$

For an $N \times N$ circulant H, representing the convolution of an $N \times 1$ signal with the kernel

$$\ldots h(-2), h(-1), h(0), h(1), h(2) \ldots \tag{20}$$

centered at 0, it can be shown that

$$H_D = (D\ H\ D^T) = \begin{bmatrix} H_{(0)} & H_{(1)} \\ H_{(-1)} & H_{(0)} \end{bmatrix} \tag{21}$$

where $H_{(j)}$ is an $\frac{N}{2} \times \frac{N}{2}$ circulant matrix representing the convolution of an $\frac{N}{2} \times 1$ vector with the kernel

$$\ldots h(j-4), h(j-2), h(j), h(j+2), h(j+4) \ldots \tag{22}$$

centered at j. Thus, by applying D to the convolution operator, it is decomposed into the convolution operators $H_{(j)}$, each of half length, and simply defined by the even and odd coefficients of the original operator.

Based on the previous decomposition of H, (19) yields

$$\begin{aligned} &(\tilde{W}g_D) = (\tilde{W}H_D\tilde{W}^T)(\tilde{W}f_D) \\ \Longrightarrow\quad &\tilde{g} = (\tilde{W}H_D\tilde{W}^T)\tilde{f} = \tilde{H}\tilde{f} \end{aligned} \tag{23}$$

where $\tilde{f}$ and $\tilde{g}$ are the $\tilde{W}$ domain original and convolved signals, respectively, and $\tilde{H}$ is the transformed convolution operator. Since $\tilde{W}$ and H_D are BSC $(2, \frac{N}{2})$ matrices, $\tilde{H}$ is also a BSC $(2, \frac{N}{2})$ matrix. Therefore, the decomposition of H is also easy to compute in the DFT domain.

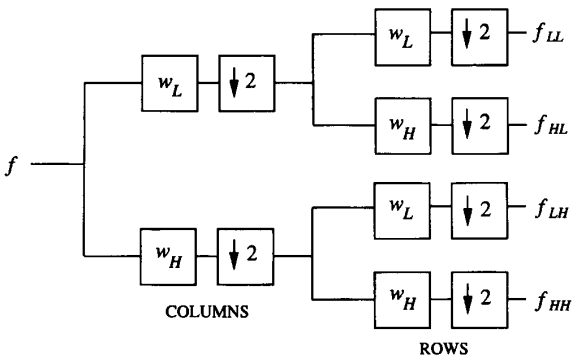

Fig. 2. Four-channel 2-D decomposition.

IV. The 2-D Separable Case

A simple 2-D decomposition can be derived, based on the previous two-channel 1-D decomposition, if w_L and w_H are applied in the horizontal and vertical directions of a 2-D signal separately. For an $N \times N$ input signal, $f(x, y)$, one level of this decomposition will yield four $\frac{N}{2} \times \frac{N}{2}$ channels, as shown in Fig. 2.

In order to represent the operations shown here using matrix vector notation, it is easier to use the BSC representation. Thus, we consider ordering the output data from this filter bank in terms of spatial indexing first, followed by the channel indexing, as in (2). In analogy to the 1-D case, (15) can be used to describe this decomposition as well. If lexicographic ordering by columns is used to stack the 2-D $N \times N$ signal into a $N^2 \times 1$ vector f, then, by following steps similar to the 1-D case, after some matrix algebra it can be shown that the vector $\tilde{f}$ is given by

$$\tilde{f} = \left[(f_{LL})^T, (f_{HL})^T, (f_{LH})^T, (f_{HH})^T\right]^T \tag{24}$$

where f_{ij}, with $i, j = L, H$, are the four $\frac{N}{2} \times \frac{N}{2}$ 2-D channels lexicographically ordered by columns. The indices i and j correspond to filtering along the x and y directions, respectively, i.e., f_{HL} is the channel obtained by highpass filtering in the x direction and lowpass filtering in the y direction. The vector f_D in the 2-D case is given by

$$f_D = \left[(f_{EE})^T, (f_{OE})^T, (f_{EO})^T, (f_{OO})^T\right]^T \tag{25}$$

where f_{ij}, for $i, j = E, O$, are the four $\frac{N}{2} \times \frac{N}{2}$ 2-D subimages lexicographically ordered by columns obtained by sampling in the x and y directions, and retaining the even or odd samples. For example, f_{EO} is the $\frac{N}{2} \times \frac{N}{2}$ subimage which is obtained by selecting the pixels with even indices in the x direction and odd indices in the y direction from the original image f.

Since filtering is applied separately in the x and y directions, the matrix $\tilde{W}$ for the 2-D case is given by $\tilde{W} = \tilde{W}_x \cdot \tilde{W}_y$ where $\tilde{W}_x$ and $\tilde{W}_y$ represent the filtering in the x and y directions, respectively. Furthermore, $\tilde{W}_x$ and $\tilde{W}_y$ are $N^2 \times N^2$

matrices defined as

$$\tilde{W}_x = \begin{bmatrix} W^E{}_{(L,\,x)} & W^O{}_{(L,\,x)} & [\,0\,] & [\,0\,] \\ W^E{}_{(H,\,x)} & W^O{}_{(H,\,x)} & [\,0\,] & [\,0\,] \\ [\,0\,] & [\,0\,] & W^E{}_{(L,\,x)} & W^O{}_{(L,\,x)} \\ [\,0\,] & [\,0\,] & W^E{}_{(H,\,x)} & W^O{}_{(H,\,x)} \end{bmatrix} \tag{26}$$

where "[0]" is an $\frac{N^2}{4} \times \frac{N^2}{4}$ matrix of zeros, and the $\frac{N^2}{4} \times \frac{N^2}{4}$ matrices $W^j_{(i,x)}$, for $j = E, O$ and $i = L, H$, are defined by

$$W^j{}_{(i,x)} = W^j{}_i \otimes [I]. \tag{27}$$

Here, $\otimes$ is the Kronecker product, $\{W^j\}_i$ are the $\frac{N}{2} \times \frac{N}{2}$ circulant matrices given in (17), and $[I]$ is the $\frac{N}{2} \times \frac{N}{2}$ identity matrix. In addition

$$\tilde{W}_y = \begin{bmatrix} W^E{}_{(L,\,y)} & [\,0\,] & W^O{}_{(L,\,y)} & [\,0\,] \\ [\,0\,] & W^E{}_{(L,\,y)} & [\,0\,] & W^O{}_{(L,\,y)} \\ W^E{}_{(H,\,y)} & [\,0\,] & W^O{}_{(H,\,y)} & [\,0\,] \\ [\,0\,] & W^E{}_{(H,\,y)} & [\,0\,] & W^O{}_{(H,\,y)} \end{bmatrix} \tag{28}$$

where the $\frac{N^2}{4} \times \frac{N^2}{4}$ matrices, $W^j_{(i,y)}$, are defined by

$$W^j_{(i,y)} = [I] \otimes W^j_i. \tag{29}$$

Since the matrices $W^j_{(i,k)}$, for $i = L, H$, $j = E, O$ and $k = x, y$ are defined as Kronecker products of two $\frac{N}{2} \times \frac{N}{2}$ circulant matrices, they are $\frac{N^2}{4} \times \frac{N^2}{4}$ block circulant matrices. However, the $N^2 \times N^2$ block matrices $\tilde{W}_y$ and $\tilde{W}_x$ are not circulant. Matrices of this form, which are an extension of the 1-D case, are called block-block semi-circulant (BBSC) of order $(4, \frac{N^2}{4})$. These matrices have exactly the same properties as BSC matrices when the 2-D DFT is used for their transformation [16], [20].

The dual representation of the 2-D $\tilde{W}$ is a block semi-block circulant (BSBC) matrix W. In this case, the 2-D signal decomposition may be described by

$$WTf = \tilde{f}_I \tag{30}$$

where

$$\tilde{f}_I = \Bigg[f(0,0)_{LL}, f(0,0)_{HL}, f(0,0)_{LH}, f(0,0)_{HH}; \\ f(1,0)_{LL}, f(1,0)_{HL}, f(1,0)_{LH}, f(1,0)_{HH}; \\ \ldots, f\left(\frac{N}{2}-1, \frac{N}{2}-1\right)_{LL}, f\left(\frac{N}{2}-1, \frac{N}{2}-1\right)_{HL}, \\ f\left(\frac{N}{2}-1, \frac{N}{2}-1\right)_{LH}, f\left(\frac{N}{2}-1, \frac{N}{2}-1\right)_{HH} \Bigg]^T \tag{31}$$

Here, T is an $N^2 \times N^2$ matrix of ones and zeroes that groups every block of four neighbors of the original image into a vector. The matrix T does not appear in (8), for the 1-D case, and is a result of the lexicographic ordering that is used in the 2-D formulation. It is easy to show that $T^T T = I_{N^2 \times N^2}$. For a detailed treatment of the 2-D BSBC formulation, see [25]–[27].

In two dimensions, the decomposition of the block circulant convolution operator H is easier to follow using the BBSC notation. Let us assume that H is an $N^2 \times N^2$ block circulant matrix representing the circular 2-D convolution of an $N \times N$ signal with the following mask, which is centered at $(0, 0)$, see (32) at the bottom of this page. If steps similar to those taken in the 1-D case are followed, then after some tedious matrix algebra, it can be shown that (23) holds true for the 2-D case also. Then, $\tilde{g}$ is an $N^2 \times 1$ vector of the same form as $\tilde{f}$ in (24). Furthermore, H_D is given by

$$H_D = \begin{bmatrix} H_{(0,\,0)} & H_{(-1,\,0)} & H_{(0,\,1)} & H_{(-1,\,1)} \\ H_{(1,\,0)} & H_{(0,\,0)} & H_{(1,\,1)} & H_{(0,\,1)} \\ H_{(0,\,-1)} & H_{(-1,\,-1)} & H_{(0,\,0)} & H_{(-1,\,0)} \\ H_{(1,\,-1)} & H_{(0,\,-1)} & H_{(1,\,0)} & H_{(0,\,0)} \end{bmatrix} \tag{33}$$

where $H_{(i,j)}$ are $\frac{N^2}{4} \times \frac{N^2}{4}$ block circulant matrices that represent the circular 2-D convolution of an $\frac{N}{2} \times \frac{N}{2}$ 2-D signal with the mask

$$\begin{matrix} \cdot & \cdot & \cdot & \cdot \\ \cdot & \cdot & \cdot & \cdot \\ \cdot & h(i-2,\,j+4) & h(i,\,j+4) & h(i+2,\,j+4) & \cdot \\ \cdot & h(i-2,\,j+2) & h(i,\,j+2) & h(i+2,\,j+2) & \cdot \\ \cdot & h(i-2,\,j) & h(i,\,j) & h(i+2,\,j) & \cdot \\ \cdot & h(i-2,\,j-2) & h(i,\,j-2) & h(i+2,\,j-2) & \cdot \\ \cdot & h(i-2,\,j-4) & h(i,\,j-4) & h(i+2,\,j-4) & \cdot \\ \cdot & \cdot & \cdot & \cdot \\ \cdot & \cdot & \cdot & \cdot \end{matrix} \tag{34}$$

centered at $(i,\ j)$.

From (33) it is clear that H_D is also a BBSC $(4, \frac{N^2}{4})$ matrix. Furthermore, since (23) holds for the 2-D case also, $\tilde{H}$ is a BBSC $(4, \frac{N^2}{4})$ matrix. Therefore, the beneficial frequency domain properties of $\tilde{H}$ are preserved in the 2-D case. In the case of the BSBC formulation, the computation involves terms defined by $WTHT^TW^T$. The matrix THT^T is BSBC, and thus this product may be computed with block diagonal matrices in the DFT domain [25]–[27].

$$\begin{matrix} \cdot & \cdot & \cdot & \cdot & \cdot & \cdot \\ \cdot & \cdot & \cdot & \cdot & \cdot & \cdot \\ \cdot & h(-2,\,2) & h(-1,\,2) & h(0,\,2) & h(1,\,2) & h(2,\,2) & \cdot \\ \cdot & h(-2,\,1) & h(-1,\,1) & h(0,\,1) & h(1,\,1) & h(2,\,1) & \cdot \\ \cdot & h(-2,\,0) & h(-1,\,0) & h(0,\,0) & h(1,\,0) & h(2,\,0) & \cdot \\ \cdot & h(-2,\,-1) & h(-1,\,-1) & h(0,\,-1) & h(1,\,-1) & h(2,\,-1) & \cdot \\ \cdot & h(-2,\,-2) & h(-1,\,-2) & h(0,\,-2) & h(1,\,-2) & h(2,\,-2) & \cdot \\ \cdot & \cdot & \cdot & \cdot & \cdot & \cdot \\ \cdot & \cdot & \cdot & \cdot & \cdot & \cdot \end{matrix} \tag{32}$$

Fig. 3. The original 256 × 256 "Lena" image.

V. Multichannel LMMSE Filtering in the $\tilde{W}$ Domain

The previously described decomposition can be used to transform any single-channel linear space-invariant filtering problem into a multichannel one. We have applied this decomposition to the LMMSE space-invariant formulation of the image restoration problem. Using similar steps, the same decomposition can be applied also to a variety of other problems, such as the constrained least squares formulation of the image restoration problem, or image reconstruction from projections [28].

The LMMSE restoration filter is given by

$$\hat{f} = R_{ff}\, H^T (H\, R_{ff}\, H^T + R_{nn})^{-1}\, g \tag{35}$$

when (1) is used as the imaging equation, the means of the noise and original image are zero, and the noise is uncorrelated with the original signal. Here $R_{ff} = E\{ff^T\}$, represents the auto-correlation of the original image, and $R_{nn} = E\{nn^T\}$ represents the auto-correlation of the noise [18]. For realistic images, the size of H, R_{ff}, and R_{nn} is extremely large. For example, 256 × 256 images would result in 65 536 × 65 536 matrices. Therefore, a global stationarity assumption is generally used, thus making R_{ff} and R_{nn} block circulant [18]. The computation of (35) can then be performed in the DFT domain [18].

The development in Section IV leads directly to a consideration of this problem in the $\tilde{W}$ domain. In this section, we will refer to the decomposition in terms of BBSC matrix structures, but the techniques using BSBC structures are directly applicable as well [25]–[27]. The transformation of (35) into the $\tilde{W}$ domain yields

$$\begin{aligned}(\tilde{W}D)\hat{f} &= (\tilde{W}D)\left[R_{ff}H^T(HR_{ff}H^T + R_{nn})^{-1}g\right] \\ &= R_{\tilde{f}\tilde{f}}\tilde{H}(\tilde{H}R_{\tilde{f}\tilde{f}}\tilde{H}^T + R_{\tilde{n}\tilde{n}})^{-1}\tilde{g}\end{aligned} \tag{36}$$

where $R_{\tilde{f}\tilde{f}} = E\left\{\tilde{f}\tilde{f}^T\right\}$, and $R_{\tilde{n}\tilde{n}} = E\{\tilde{n}\tilde{n}^T\}$ are the auto-correlation matrices of the original signal and the noise in the $\tilde{W}$ domain. Examining for a moment the problem of 1-D signal restoration, in which f is decomposed into two channels, we would have

$$R_{\tilde{f}\tilde{f}} = \begin{bmatrix} R_{LL} & R_{LH} \\ R_{HL} & R_{HH} \end{bmatrix} \tag{37}$$

where $R_{ij} = E\{f_i f_j^T\}$, for $i,j = L,H$. For $i = j$, R_{ij} describes the auto-correlation of the two channels, and for $i \neq j$, it describes the cross-correlation. Because within-channel stationarity is assumed, each of the $\frac{N}{2} \times \frac{N}{2}$ matrices is circulant. However, since stationarity between channels is not assumed, the $N \times N$ matrix $R_{\tilde{f}\tilde{f}}$ is not circulant, but rather a BSC $(2, \frac{N}{2})$ matrix. Therefore, the filter in (36) can be computed in the DFT domain using the methods presented in [16], [21], and [22]. The 2-D case is equivalent in terms of matrix structures, only this decomposition results in four channels, or BBSC$(4, \frac{N^2}{4})$ matrices.

The main advantage of this formulation is that it allows for the removal of the global stationarity assumption that is traditionally used in LMMSE image restoration [18]. Since each of the $\frac{N^2}{4} \times \frac{N^2}{4}$ R_{ij} matrices that appears in the 2-D case is block circulant, but $R_{\tilde{f}\tilde{f}}$ is not, what we have effectively achieved is a reduction of the assumed stationarity length in our image model from N to $\frac{N}{2}$. Thus, $R_{\tilde{f}\tilde{f}}$ can be used to capture the image properties more accurately, and therefore, multichannel restoration in the $\tilde{W}$ domain may reduce some of the "traditional" artifacts of stationary image restoration. These artifacts include ringing, oversmoothing of edges and filtered noise effects in flat regions of the image.

The transformation of a single-channel problem into a four-channel problem seen here is only one potential approach to using the matrix $\tilde{W}$. Since the more channels used for the decomposition the smaller the stationarity length assumed, we transformed the four-channel problem into a 16–channel one where the stationarity length was reduced to $\frac{N}{4}$. This was accomplished by taking each of the terms in the four-channel problem and transforming it into a four-channel term itself. It is relatively straightforward to see that this can be accomplished simply by multiplying the result of the first filter bank operation with a matrix implicitly containing four smaller support $\tilde{W}$ matrices to produce a result having 16 channels. This matrix may be written simply as a BBSC $(16, \frac{N^2}{16})$ matrix, or it could be written in dual form as BSBC with a block diagonal frequency domain counterpart having subblocks of support 16 × 16.

VI. Experimental Results

In a sequence of experiments, the proposed multichannel approach was tested. The original 256 × 256 "Lena" image, shown in Fig. 3, was blurred by an 11 × 11 uniform blur and then degraded by additive noise to achieve 20, 30, and 40 dB in blurred signal-to-noise ratio (BSNR). The resulting degraded images are shown in Figs. 4(a), 5(a), and 6(a), respectively. The degraded images were first restored using the classical single-channel LMMSE (Wiener) filter [18], and

Fig. 4. (a) The degraded "Lena" image with 11 × 11 blur and 20 dB of additive noise; (b) the restored image obtained by using the traditional one-channel LMMSE filter (ISNR = 3.39 dB); (c) the restored image obtained by using a four-channel wavelet-based multichannel LMMSE filter, (ISNR = 3.89 dB); (d) The restored image obtained by using a 16-channel wavelet-based multichannel LMMSE filter, (ISNR = 6.55 dB).

the resulting restored images are shown in Figs. 4(b), 5(b), and 6(b). Next, the degraded images were restored by the proposed multichannel LMMSE filter given in (36) using a 4- and 16-channel decomposition. This decomposition was implemented using the Daubechies 16-wavelet basis [24]. The resulting restored images from the multichannel filters are shown in Figs. 4(c)–(d), 5(c)–(d), and 6(c)–(d). For both the single and multichannel approaches the required statistics were estimated from the original image and the original image subbands, using the periodogram approach. The choice of the 16-tap wavelet filter is motivated by the high regularity of this wavelet, which causes most of the important structural information in the image to be projected into the lowest frequency subbands. We have, however, performed the same experiments with other orthogonal wavelet filters, namely the Daubechies 4-, 8-, and 20-tap filters. In all experiments, the restored images are indistinguishable. In other words, the results are largely independent of the choice of QMF, as long as the perfect reconstruction property is met, which is a requirement of the theory developed here. This independence of the wavelet filter stems from the fact that the correlation information used to produce the results is not degraded by choosing different filters. We merely remap this correlation information differently, placing more signal energy in the

Fig. 5. (a) The degraded "Lena" image with 11×11 blur and 30 dB of additive noise; (b) the restored image obtained by using the traditional one–channel LMMSE filter (ISNR = 5.07 dB); (c) The restored image obtained by using a four-channel wavelet-based multichannel LMMSE filter (ISNR = 6.01 dB); (d) The restored image obtained by using a 16-channel wavelet-based multichannel LMMSE filter (ISNR = 10.42 dB).

high frequency subbands when using less regular wavelets. All useful cross- and auto-correlation information which leads to the multichannel restoration filter is still maintained with different filters, but it is simply projected differently into the subband space.

Both the BSBC and BBSC formulations have been used to implement these multichannel filters using spatial and frequency domain approaches in computing the multichannel linear operators, respectively. For the spatial implementation, a simple modification which involves removing T from (30) and reordering the columns of W appropriately, explicitly encourages the use of spatial convolutions and decimations for the computation of H or any other block circulant matrix, in the W domain. This is an efficient and fast approach to solving linear filtering problems in the subband domain. It allows the use of spatial QMF bank implementations to be used repetitively on an operator such as H, so that eight applications of this filter bank will compute the BSBC expression $WTHT^TW^T$ [25]–[27].

As an objective measure of performance, the improvement in signal-to-noise ratio (ISNR) was used. This may be defined in dB as

$$\text{ISNR} = 20 \log \left\{ \frac{\|f - g\|}{\|f - \hat{f}\|} \right\} \tag{38}$$

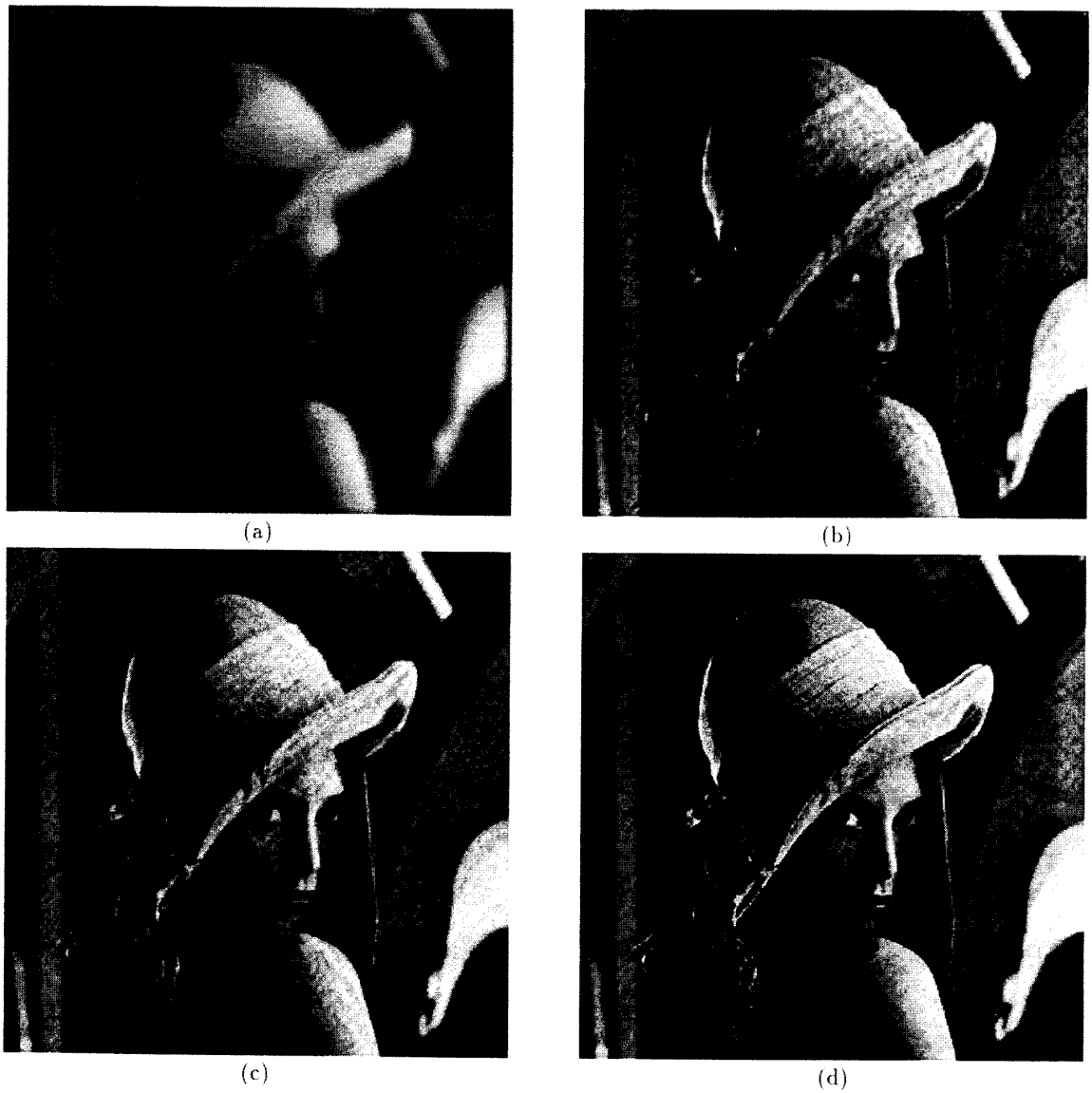

Fig. 6. (a) The degraded "Lena" image with 11 × 11 blur and 40 dB of additive noise; (b) the restored image obtained by using the traditional one-channel LMMSE filter (ISNR = 7.10 dB); (c) The restored image obtained by using a four-channel wavelet-based multichannel LMMSE filter (ISNR = 8.88 dB); (d) the restored image obtained by using a 16-channel wavelet-based multichannel LMMSE filter (ISNR = 16.05 dB).

TABLE I
ISNR RESULTS OBTAINED FOR THE "LENA" IMAGE, DEGRADED BY AN 11 × 11 2-D UNIFORM BLUR, USING THE CLASSICAL SINGLE CHANNEL, AND THE 4- AND 16-CHANNEL WAVELET-BASED LMMSE FILTERS

	ISNR(dB)		
BSNR (dB)	1 Channel	4 Channel	16 Channel
40	7.10	8.88	16.05
30	5.07	6.01	10.42
20	3.39	3.89	6.55

where f, g, and $\hat{f}$ are the original, degraded, and restored images, respectively. The ISNR results of the previous experiments are listed in Table I. From the images in Figs. 4–6, and the ISNR results of Table I, it is clear that the proposed multichannel restoration approach provides significant improvements both objectively, based on the ISNR metric, and also subjectively, over the traditional single channel approach for all BSNR levels. The experimental results in this section also show that further reduction of the stationarity length from $\frac{N}{2}$ (4-channels) to $\frac{N}{4}$ (16-channels) was very beneficial. In order to demonstrate the effectiveness of this algorithm at low SNR, Fig. 7 shows the degraded and restored subbands of the 20 dB BSNR case seen in Fig. 4. In particular, the subbands for the 4- and 16-channel restoration algorithms are shown here. For comparison purposes, the same subbands are seen

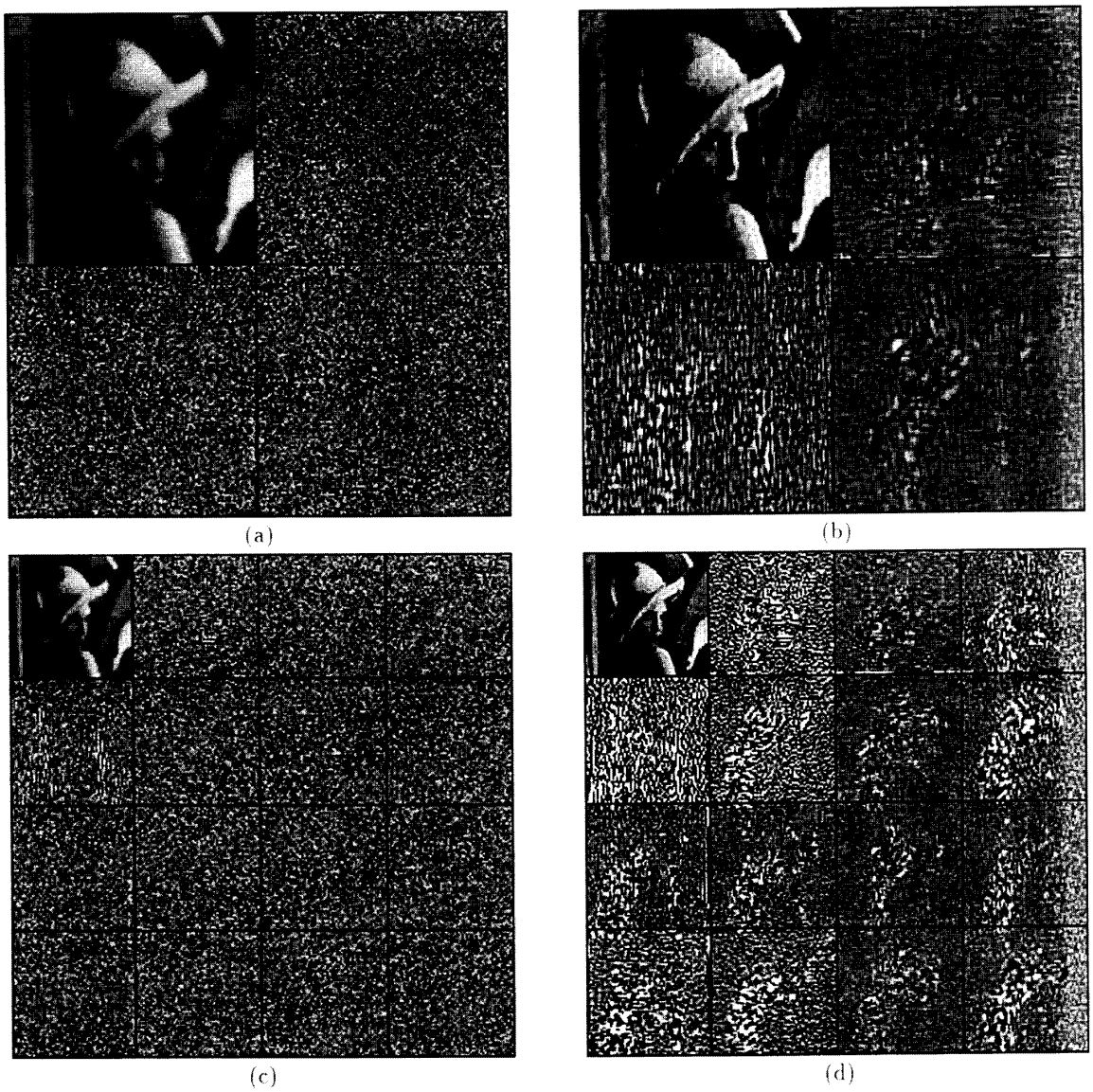

Fig. 7. (a) Subbands of the degraded "Lena" image with 11×11 blur and 20 dB of additive noise, four channels; (b) subbands of the restored image obtained by using a 4-channel wavelet-based multichannel LMMSE filter; (c) Subbands of the degraded "Lena" image with 11×11 blur and 20 dB of additive noise, 16-channels; (d) Subbands of the restored image obtained by using a 16-channel wavelet-based multichannel LMMSE filter.

for the 40 dB BSNR case in Fig. 8. It is clear, in both cases, that the structure is restored not only in the low frequency subbands where the SNR is high, but also in the high frequency subbands, where the noise dominates. This good restoration is largely due to the accurate cross subband correlations used in generating the restored images in the multichannel wavelet domain.

VII. Conclusion and Future Research

In this paper, we presented a new matrix vector formulation for the subband decomposition of linear space-invariant filtering problems. This formulation allows for the efficient transformation of any linear space-invariant filtering problem to a multichannel one. Subband decomposition is a well established method for compressing both speech and image signals [12], [29]. We showed that another application, image restoration, can also benefit from this transformation. Here, a subband decomposition was used to relax the stationarity assumption which is traditionally imposed in linear space-invariant image restoration. More specifically, we combined the LMMSE formulation of the restoration problem with the proposed decomposition to obtain a family of multichannel

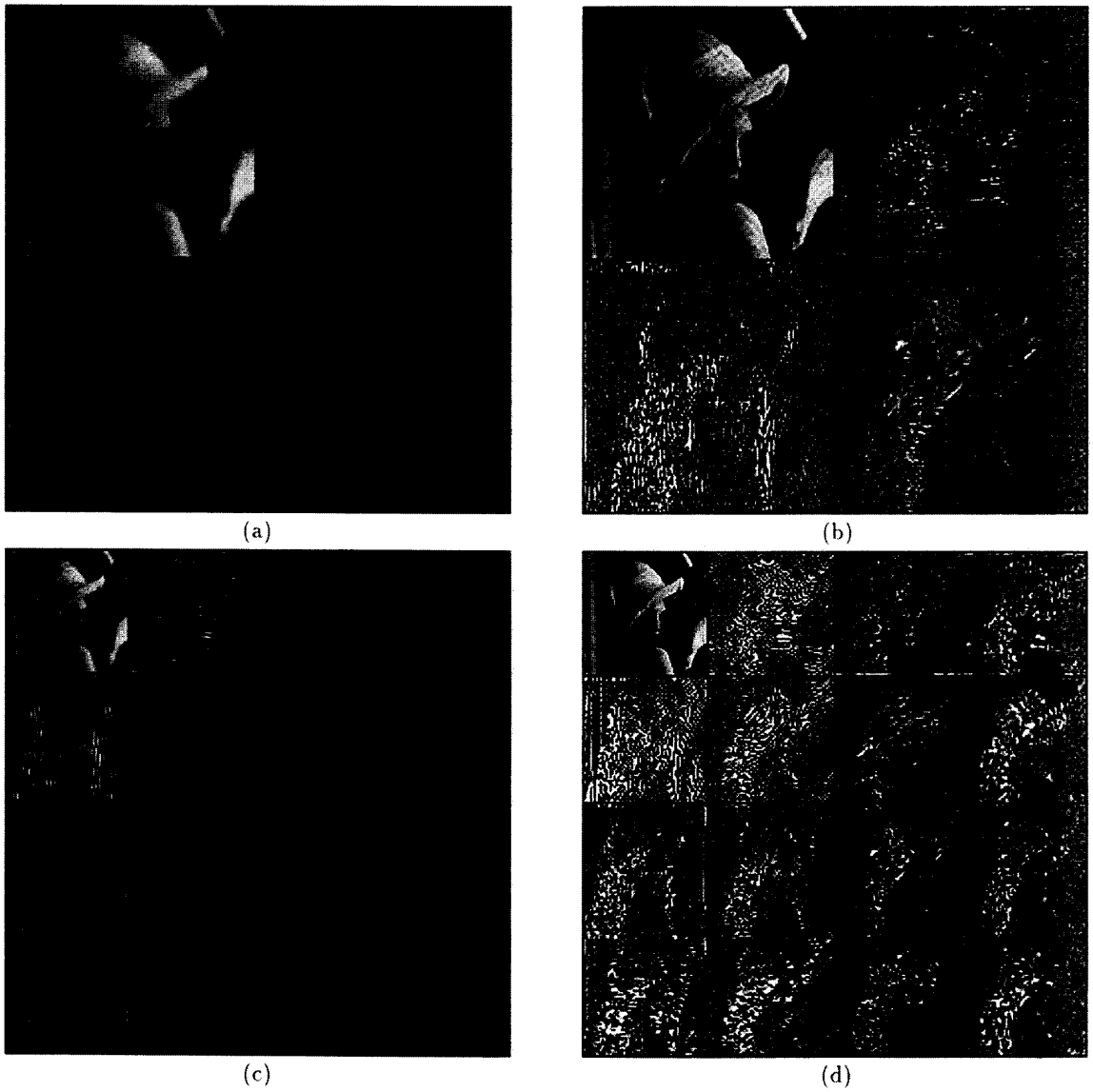

Fig. 8. (a) Subbands of the degraded "Lena" image with 11 × 11 blur and 40 dB of additive noise, 4-channels; (b) Subbands of the restored image obtained by using a 4-channel wavelet-based multichannel LMMSE filter; (c) subbands of the degraded "Lena" image with 11 × 11 blur and 40 dB of additive noise, 16-channels; (d) subbands of the restored image obtained by using a 16-channel wavelet-based multichannel LMMSE filter.

LMMSE restoration filters. Our experimental results show that these filters have the potential to provide major improvements over traditional single-channel restoration. It is important to recognize that the reason the improvement is obtained in the wavelet domain stems from replacing the information in each auto and cross term in the wavelet domain correlation matrix. This yields a different filter than that of the single-channel LMMSE filter. This different filter uses additional information that is not present in the single channel LMMSE filter, namely the correlations between different channels which are of shorter support than the full image. So, it is the benefits of the semi-block circulant structure, and the effective use of "more information" than we have in the stationary LMMSE case, that result in increased sharpness and a reduction in restoration artifacts in the restored images seen here.

While the intent of this paper is to show the optimal case solution in the wavelet domain, and present the necessary theory to pursue other multichannel wavelet restoration techniques, we have investigated the application of multichannel spectral estimation techniques as a preliminary approach to solving this problem when only the degraded image is available. In

this case, the estimation of the cross-subband statistics, using traditional approaches for estimating the auto-correlation, turns out to be a formidable problem. We have observed minor improvements over the single-channel LMMSE filter using the multichannel EM algorithm [20] to estimate the required wavelet domain spectra. The problem is, however, very sensitive to the noisy correlation estimates, and thus alternative estimation techniques will be required to obtain further improvements in the wavelet domain.

Another avenue which we are investigating involves the use of deterministic constraints instead of stochastic constraints imposed in the multichannel wavelet domain [22], [30]. This approach circumvents the need to estimate the cross-channel spectra from noisy data, but it also provides us with less information about the true behavior of the signal. Nonetheless, we have observed some benefits to applying an iterative constrained least squares filter in this domain, including the ability of acquire a smoother image at convergence than that obtained in the single-channel equivalent technique. Both the stochastic and deterministic approaches, along with the results obtained in the optimal case presented here, provide us with ample incentive to continue investigating multichannel image restoration within the wavelet formulation described in this paper.

REFERENCES

[1] A. K. Katsaggelos, editor, *Digital Image Restoration.* New York: Springer-Verlag, 1991.

[2] G. Anderson and A. Netravali, "Image restoration based on a subjective criterion," *IEEE Trans. Syst., Man, Cybern.*, vol. CMS-6, pp. 845–853, Dec. 1976.

[3] A. K. Katsaggelos *et al.*, "Nonstationary iterative image restoration," *IEEE Proc. ICASSP*, 1985, pp. 696–699.

[4] A. K. Katsaggelos *et al.*, "A regularized iterative image restoration algorithm," *IEEE Trans. Signal Processing*, vol. 39, pp. 914–929, Apr. 1991.

[5] H. Knutsson, R. Wilson, and G. Granlund, "Anisotropic nonstationary image estimation and its applications, part I: Restoration of noisy images," *IEEE Trans. Commun.*, vol. COM-31, no. 3, pp. 388–397, Mar. 1983.

[6] S. Rajala and R. De Figueiredo, "Adaptive nonlinear image restoration by a modified Kalman filtering approach," *IEEE Trans. Acoust., Speech, Signal Processing*, vol. ASSP-29, pp. 1033–1042, Oct. 1981.

[7] J. W. Woods, "Two-dimensional Kalman filtering," in *Two-Dimensional Digital Signal Processing I*, Topics in Applied Physics, T. S. Huang, Ed. Berlin: Springer, 1981, vol. 42.

[8] F. Jeng and J. W. Woods, "Inhomogeneous Gaussian image models for estimation and restoration," *IEEE Trans. Acoust., Speech, Signal Proc.*, vol. ASSP-36, pp. 1305–1312, Aug. 1988.

[9] R. Chellapa, T. Simchony, and Z. Lichtenstein, "Image estimation using 2D Gauss-Markov random field models," in *Digital Image Restoration*, A. K. Katsaggelos, Ed. New York: Springer-Verlag, 1991.

[10] S. Geman and D. Geman, "Stochastic relaxation, Gibbs distribution, and the Bayesian restoration of images," *IEEE Trans. Pattern Anal. Machine Intell.*, vol. PAMI-6, pp. 228–238, Nov. 1984.

[11] F. Jeng and J. W. Woods, "Compound Gauss-Markov random fields for image estimation," *IEEE Trans. Signal Processing*, vol. 39, pp. 683–697, Mar. 1991.

[12] J. W. Woods, Ed., *Subband Image Coding.* Boston: Kluwer, 1991.

[13] J. Bruneau, M. Barlaud, and P. Mathieu, "Image restoration using biorthogonal wavelet transform," *SPIE Conf. Visual Commun., Image Processing*, pp. 1404–1415, Nov. 1990.

[14] P. Charbonnier, L. Blanc-Féraud, and M. Barlaud, "Noisy image restoration using multiresolution Markov random fields," *J. Visual Commun. and Image Rep.*, vol. 3, pp. 338–346, Dec. 1992.

[15] J. W. Woods and J. Kim, "Image identification and restoration in the subband domain," *IEEE Proc. ICASSP*, Mar. 1992, vol. III, pp. 297–300.

[16] N. P. Galatsanos and R. Chin, "Digital restoration of multichannel images," *IEEE Trans. Acoust., Speech, Signal Proc.*, vol. 37, pp. 415–421, March 1989.

[17] B. R. Hunt and O. Kübler, "Karhunen-Loeve multispectral image restoration, part I: Theory," *IEEE Trans. Acoust., Speech, Signal Proc.*, vol. 32, pp. 592–599, June 1984.

[18] H. C. Andrews and B. R. Hunt, *Digital Image Restoration.* Englewood Cliffs, NJ: Prentice-Hall, 1977.

[19] D. E. Dudgeon and R. M. Mersereau, *Multidimensional Digital Signal Processing.* Englewood Cliffs, NJ: Prentice Hall, 1984.

[20] K. T. Lay, "Maximum likelihood iterative image identification and restoration," Ph.D. thesis, Northwestern University, Dec. 1991.

[21] A. K. Katsaggelos, K. T. Lay, and N. P. Galatsanos, "A general framework for frequency domain multichannel signal processing," *IEEE Trans. Image Proc.*, vol. 2, pp. 417–420, July 1993.

[22] N. P. Galatsanos *et al.*, "Least squares restoration of multichannel images," *IEEE Trans. Acoust., Speech, Signal Proc.*, vol. 39, pp. 2222–2236, Oct. 1991.

[23] P. P. Vaidyanathan, *Multirate Systems and Filter Banks.* Englewood Cliffs, NJ: Prentice Hall, 1993.

[24] I. Daubechies, "Orthonormal bases of compactly supported wavelets," *Commun. Pure Appl. Math.*, vol. 41, pp. 909–996, Nov. 1988.

[25] M. R. Banham *et al.*, "Restoration of single channel images with multichannel filtering in the wavelet domain," *Proc. IEEE Int'l. Conf. Syst., Man Cybern.* (Chicago), Oct. 1992, pp. 1558–1563.

[26] M. R. Banham *et al.*, "Multichannel restoration of single channel images using a wavelet decomposition," *IEEE Proc. ICASSP* (Minneapolis), Apr. 1993, vol. V, pp. 281–284.

[27] M. R. Banham, "Wavelet-Based Image Restoration Techniques," Ph.D. thesis, Northwestern Univ., June, 1994.

[28] A. K. Jain, *Fundamentals of Digital Image Processing.* Englewood Cliffs, NJ: Prentice Hall, 1989.

[29] N. S. Jayant and P. Noll, *Digital Coding of Waveforms.* Englewood Cliffs, NJ: Prentice Hall, 1984.

[30] W. Zhu, N. P. Galatsanos, and A. K. Katsaggelos, "Regularized multichannel image restoration using cross validation," *VCIP-92, SPIE-Proc.*, Nov. 1992, vol. 1818, pp. 345–356.

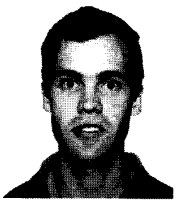

Mark R. Banham (S'87–M'94) was born in Philadelphia, PA in 1966. He received the B.S.E.E. degree from Drexel University, Philadelphia, in 1989, and the M.S. and Ph.D. degrees in electrical engineering from Northwestern University, Evanston, IL, in 1990 and 1994, respectively.

During the period from 1989 to 1994, he served as a Murphy Fellow, a Teaching Assistant, an Instructor, and a Research Assistant, all in the EECS Dept. at Northwestern. He is currently a Senior Engineer in the Digital Technology Research Laboratory of Motorola Corporate Research and Development, Schaumburg, IL. His research interests are primarily in multiresolution approaches to image restoration, still image compression, and video coding.

Dr. Banham is a member of Tau Beta Pi and Eta Kappa Nu.

Nikolas P. Galatsanos (S'89–M'89) was born in Athens, Greece in 1958. He received his diploma degree in electrical engineering from the National Technical University of Athens in 1982. He received the M.S. and the Ph.D. degrees, both in electrical and computer engineering, from the University of Wisconsin-Madison, in 1984 and 1989, respectively.

Since August 1989, he has been on the faculty of the Department of Electrical and Computer Engineering at the Illinois Institute of Technology, Chicago IL, where he is now an Assistant Professor. His current research interests include image processing and multidimensional signal processing and more specifically recovery, and compression of single and multichannel/frame images. Dr. Galatsanos presently serves as an associate editor for the IEEE TRANSACTIONS ON IMAGE PROCESSING.

Hector L. Gonzalez (M'91) was born in Aguada, Puerto Rico in 1958. He received the B.S. degree from the University of Puerto Rico in 1982, and the M.S. degree from Massachusetts Institute of Technology in 1984, all in electrical engineering. In 1989 he received the M.S. in computer science from the Illinois Institute of Technology. Currently he is Ph.D. candidate at the Department of Electrical and Computer Engineering at the Illinois Institute of Technology.

Since 1984 he has been employed by the Fermi National Accelerator Laboratory. His current research interests are in the general area of signal and image processing and in the design and development of data acquisition systems for high-energy physics experiments.

Aggelos K. Katsaggelos (S'80–M'85–SM'92) received the diploma degree in electrical and mechanical engineering from the Aristotelian University of Thessaloniki, Thessaloniki, Greece, in 1979, and the M.S. and Ph.D. degrees, both in electrical engineering, from the Georgia Institute of Technology, Atlanta, in 1981 and 1985, respectively.

In 1985, he joined the Department of Electrical Engineering and Computer Science at Northwestern University, Evanston, IL, where he is currently an Associate Professor. During the 1986-1987 academic year he was an Assistant Professor at Polytechnic University, Department of Electrical Engineering and Computer Science, Brooklyn, NY. His current research interests include image recovery, processing of moving images (motion estimation, enhancement, very low bit-rate compression), and computational vision. Dr. Katsaggelos is an Ameritech Fellow and a member of the Associate Staff, Department of Medicine, at Evanston Hospital.

He is a member of SPIE, the Steering Committees of the IEEE TRANSACTIONS ON MEDICAL IMAGING and the IEEE TRANSACTIONS ON IMAGE PROCESSING, the IEEE Technical Committees on Visual Signal Processing and Communications and on Image and Multi-Dimensional Signal Processing, the Technical Chamber of Commerce of Greece and Sigma Xi. He has served as an Associate editor for the IEEE TRANSACTIONS ON SIGNAL PROCESSING (1990–1992), and is currently an area editor for the journal *Graphical Models and Image Processing*. He is the editor of *Digital Image Restoration* (Springer-Verlag, Heidelberg, 1991) and the General Chairman of the 1994 Visual Communications and Image Processing Conference (Chicago, IL).